

Quantum Computation of Electronic Transitions Using a Variational Quantum Eigensolver

Robert M. Parrish,^{1,2,3,*} Edward G. Hohenstein,^{1,2} Peter L. McMahon,^{4,3} and Todd J. Martínez^{1,2}

¹*Department of Chemistry and the PULSE Institute, Stanford University, Stanford, California, 94305, USA*

²*SLAC National Accelerator Laboratory, Menlo Park, California, 94025, USA*

³*QC Ware Corporation, Palo Alto, California 94301, USA*

⁴*E. L. Ginzton Laboratory, Stanford University, Stanford, California, 94305, USA*

 (Received 4 January 2019; revised manuscript received 10 April 2019; published 12 June 2019)

We develop an extension of the variational quantum eigensolver (VQE) algorithm—multistate contracted VQE (MC-VQE)—that allows for the efficient computation of the transition energies between the ground state and several low-lying excited states of a molecule, as well as the oscillator strengths associated with these transitions. We numerically simulate MC-VQE by computing the absorption spectrum of an *ab initio* exciton model of an 18-chromophore light-harvesting complex from purple photosynthetic bacteria.

DOI: [10.1103/PhysRevLett.122.230401](https://doi.org/10.1103/PhysRevLett.122.230401)

The accurate modeling of the many-body interactions in the ground- and excited-state solutions of the electronic Schrödinger equation is a prerequisite for the quantitative prediction of molecular physical phenomena such as light harvesting. Using classical computers, this problem scales formally as the factorial of the number of involved electrons [1], via the solution of the full configuration interaction (FCI) equations, though many polynomial-scaling approximations such as density functional theory [2–5] (DFT), coupled cluster theory [6–9] (CC), density matrix renormalization group [10,11] (DMRG), adaptive and/or stochastic configuration interaction methods [12–18] (CIPSI and variants), and semistochastic coupled cluster methods [19,20] have been developed to combat this problem. Recently, there has been a surge of interest in using quantum computers to naturally solve the many-body electronic structure problem through methods such as the iterative phase estimation algorithm [21–26] (IPEA) or the variational quantum eigensolver [27–32] (VQE). However, the quartic-scaling complexity in number of molecular orbitals of the second-quantized electronic Hamiltonian, coupled with the overhead of encoding the fermionic antisymmetry of the electrons through the Jordan-Wigner [33,34], Bravyi-Kitaev [35,36], or superfast Bravyi-Kitaev [37,38] transformations, implies that rather long circuit depths will be required to directly model the electronic structure problem. We also point out a recent approach [39–41] that might formally reduce this complexity to quadratic or linear via a tensor hypercontraction representation [42–44] of the potential. In the present work, we explore a domain- and problem-specific means to reduce the complexity of the representation of the electronic structure problem in quantum computing: an *ab initio* exciton model [45–49]. For large-scale photoactive

complexes consisting of a number of nonbonded chromophore units, the *ab initio* exciton model compresses the details of the electronic structure on each chromophore into a handful of monomer electronic states. The determination of the full configuration interaction wave functions describing the mixing of monomer electronic states in the full complex remains a formidable task—here we show that this might be a natural computational task for a near-term quantum computer.

Another area that deserves exploration is the development of efficient quantum algorithms for the even-handed treatment of ground- and excited-state energies and transition properties, e.g., for the computation of absorption spectra. There exist IPEA-type algorithms for excited states, such as the witness-assisted variational eigenspectra solver protocol [50] or the variational swap test [51], but we focus on VQE-type methods here. Most existing VQE-type quantum algorithms are “state specific,” meaning that they optimize the VQE parameters for one state at a time. Examples include the folded spectrum method [27], which requires the observation of the square of the Hamiltonian, or the orthogonality-constrained VQE method [52,53], which applies a penalty term to remove contaminants from lower-lying states. Another, more-global approach is the quantum subspace expansion (QSE-VQE) [54,55], which first performs VQE to determine the ground state, and then determines the excited states by classical diagonalization on a basis of response states. QSE-VQE treats all the excited states on a similar footing, but by construction favors the ground state, and requires the determination of three- and four-particle density matrices through high-order Pauli measurements.

MC-VQE.—Inspired by the mixed quantum-classical strategy of QSE-VQE (particularly the final classical

diagonalization step), we have developed a new multistate contracted variant of VQE (MC-VQE), which aims to (1) treat the ground and a handful of excited states on the same footing, (2) minimize the size of the classical subspace that must be diagonalized, and (3) provide for the straightforward computation of transition properties such as oscillator strengths. MC-VQE takes the following ansatz for a number (N_Θ) of eigenstates of interest

$$|\Psi_\Theta\rangle \equiv \hat{U} \sum_{\Theta'} |\Phi_{\Theta'}\rangle V_{\Theta'\Theta}. \quad (1)$$

Here $|\Phi_\Theta\rangle$ are a set of contracted, orthonormal “reference” states, which are obtained by solving a classical electronic structure problem such as configuration interaction singles (CIS). By contracted, we mean that these reference states are generally taken to be a linear combination of Hilbert-space configurations—ideally this will allow the reference states to be reasonably accurate approximations to the exact eigenstates. As will be seen, all that we will require is that we have an efficient quantum circuit to prepare the “diagonal” state $|\Phi_\Theta\rangle$ and the “interfering” state $(|\Phi_\Theta\rangle \pm |\Phi_{\Theta'}\rangle)/\sqrt{2}$. For CIS reference states, this is possible—see the Supplemental Material [56] for a detailed circuit which generalizes a previously known circuit for $|W_N\rangle$ states [57].

The operator $\hat{U}(\{\eta\})$ is the VQE entangler matrix, an orthogonal Hilbert-space matrix constructed from a set of two-qubit entangling operators whose set of parameters $\{\eta\}$ will be chosen to maximally decouple $\{|\Phi_{\Theta'}\rangle\}$ from the rest of the Hilbert space, i.e., to approximately block diagonalize the Hamiltonian. The matrix $V_{\Theta'\Theta}$ is an $N_\Theta \times N_\Theta$ orthogonal matrix that describes the rotation of the entangled contracted states $\{|\chi_{\Theta'}\rangle \equiv \hat{U}|\Phi_{\Theta'}\rangle\}$ to the approximate eigenbasis $\{|\Psi_\Theta\rangle\}$. This matrix can be determined by classical diagonalization of the entangled contracted Hamiltonian

$$H_{\Theta'\Theta} V_{\Theta'\Theta} = V_{\Theta'\Theta} E_\Theta; \quad V_{\Theta'\Theta} V_{\Theta'\Theta'} = \delta_{\Theta\Theta'}. \quad (2)$$

The eigenvalues E_Θ are the Ritz approximations to the exact eigenvalues. The entangled contracted Hamiltonian is

$$H_{\Theta\Theta'} \equiv \langle \Phi_\Theta | \hat{U}^\dagger \hat{H} \hat{U} | \Phi_{\Theta'} \rangle. \quad (3)$$

The diagonal matrix elements can be evaluated by partial tomography measurements in a quantum computer, as is done in standard VQE

$$H_{\Theta\Theta} = \langle \Phi_\Theta | \hat{U}^\dagger \hat{H} \hat{U} | \Phi_\Theta \rangle. \quad (4)$$

The (real) off-diagonal matrix elements can also be obtained from observable quantities

$$2H_{\Theta\Theta'} = (\langle \Phi_\Theta | + \langle \Phi_{\Theta'} |) \hat{U}^\dagger \hat{H} \hat{U} (|\Phi_\Theta\rangle + |\Phi_{\Theta'}\rangle) / 2 \\ - (\langle \Phi_\Theta | - \langle \Phi_{\Theta'} |) \hat{U}^\dagger \hat{H} \hat{U} (|\Phi_\Theta\rangle - |\Phi_{\Theta'}\rangle) / 2. \quad (5)$$

This highlights the need for quantum circuits to prepare the “interfering” state $(|\Phi_\Theta\rangle \pm |\Phi_{\Theta'}\rangle)/\sqrt{2}$.

The parameters of the MC-VQE entanglement circuit should be chosen to maximally decouple the full set of approximate eigenstates $\{|\Psi_\Theta\rangle\}$ from the rest of the Hilbert space. This can be accomplished in a two-norm sense in the Hamiltonian by optimizing the parameters of the VQE entangler operator to minimize the state-averaged energy

$$\bar{E} = \frac{1}{N_\Theta} \sum_{\Theta} E_\Theta = \frac{1}{N_\Theta} \sum_{\Theta} H_{\Theta\Theta}. \quad (6)$$

The second equality follows from the definition of the trace and shows that the minimization of the state-averaged energy is equivalent to the minimization of the sum of diagonal contracted Hamiltonian matrix elements.

Overall, the MC-VQE algorithm has the following four stages: (1). Classically solve CIS or some other polynomial-scaling electronic structure problem to “sketch out” the shapes of the relevant states by determining the contracted reference states $\{|\Phi_\Theta\rangle\}$. (2). Vary the parameters of the VQE entangler operator to optimize the state-averaged energy $\bar{E} = (1/N_\Theta) \sum_{\Theta} H_{\Theta\Theta}$. (3). For the converged VQE entangler operator, observe the reference-state Hamiltonian $H_{\Theta\Theta'}$ using sums and differences of Hamiltonian expectations of interference states. (4). Classically diagonalize $H_{\Theta\Theta'}$ to obtain the Ritz estimates of the eigenstates and eigenvalues. A schematic of the quantum circuit needed to prepare a CIS state $|\Phi_\Theta\rangle$ and apply the VQE entangler \hat{U} is shown in Fig. 1—the two-body $SO(4)$ entanglers, e.g., \hat{U}_2^{AB} are constructed from known six-parameter circuit elements [58–61]—full details of this circuit are available in the Supplemental Material [56]. Overall, the MC-VQE approach has a number of

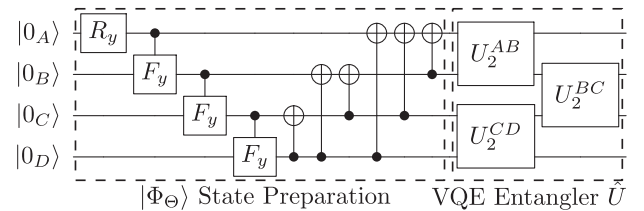


FIG. 1. Example MC-VQE quantum circuit for $N = 4$ linear exciton model. The first stage prepares contracted CIS reference states $|\Phi_\Theta\rangle$ [or interference variations $(|\Phi_\Theta\rangle \pm |\Phi_{\Theta'}\rangle)/\sqrt{2}$ thereof] specified by rotation angles in the R_y and F_y gates. The second stage applies the many-body VQE entangler \hat{U} specified through a polynomial number of rotation angles two-body U_2 entangler gates. One- and two-body Pauli measurements of this circuit then determine the entangled contracted Hamiltonian matrix elements $H_{\Theta\Theta'}$.

following unique features relative to established excited-state VQE approaches such as quantum subspace expansion (QSE-VQE) [54]: (i). The VQE entangler \hat{U} is optimized in a state-averaged manner, providing a balanced treatment of ground and excited states, i.e., all states are computed to approximately equal accuracy. (ii) The optimization of the VQE entangler \hat{U} requires only the measurement of N_Θ diagonal matrix elements $H_{\Theta\Theta}$. The determination of the N_Θ^2 off-diagonal matrix elements $H_{\Theta\neq\Theta'}$ can be done separately, after the VQE entangler parameters have been optimized. (iii) Higher-order density matrices are not required.

Note that the eigenstates can be reexpressed as $|\Psi_\Theta\rangle \equiv \hat{U}|\Gamma_\Theta\rangle$ where $\{|\Gamma_\Theta\rangle \equiv \sum_{\Theta'} |\Phi_{\Theta'}\rangle V_{\Theta'\Theta}\}$ are rotated reference states. The algorithm above is quite general—we present a demonstration below for the case of the *ab initio* exciton model, but it is clear that this approach might be immediately applicable to the efficient computation of excited states in fermionic electronic structure computations. Transition properties (such as the transition dipole moment, needed for computing the absorption spectrum) can also be computed by substituting the desired operator \hat{O} in place of \hat{H} in Eq. (5).

It is worth noting that MC-VQE can be roughly pictured either as a generator of the wave function ansatz of Eq. (1) or as a means to observe the elements of the unitarily transformed effective Hamiltonian of Eq. (4), wherein the VQE entangler operator \hat{U} acts as a wave operator [62,63].

Ab initio exciton model.—Consider a set of N chromophoric monomers, each labeled by index A , which are arranged in a particular nuclear geometry in a photoactive complex. In isolation, the chromophores are usually characterized by a constant number of photoactive electronic states, regardless of the number of electrons in the monomer (often between two and four states are photoactive in the visible spectrum in the monomer: the ground and the first few singlet excited states). If the monomers are sufficiently far apart in the full photoactive complex (e.g., if they are at noncovalent separations due to embedding in a protein scaffold), the strict considerations of fermionic antisymmetry can be relaxed without loss of accuracy, and the full complex electronic eigenstates can be computed as a configuration interaction of direct products of monomer states. That is, for electronic state Θ in a system where each chromophoric monomer is characterized by the ground state $|0_A\rangle$ and the first excited state $|1_A\rangle$ (a restriction we make from here onward to facilitate ease of mapping to qubits), the electronic states are

$$|\Psi_\Theta\rangle = \sum_{p_0, q_1, \dots \in \{0,1\}} C_{p_0 q_1 \dots r_{N-1}}^\Theta |p_0\rangle \otimes |q_1\rangle \otimes \dots \otimes |r_{N-1}\rangle. \quad (7)$$

Typically, we wish to find these adiabatic electronic states, e.g., to determine the energy gaps and oscillator strengths in

the system as a proxy for the electronic absorption spectrum. Formally, this requires diagonalization of the exciton Hamiltonian, which can straightforwardly be written in Pauli matrix notation for the special case considered here of a photoactive system with two electronic states per monomer

$$\begin{aligned} \hat{H} = \mathcal{E} + \mathcal{H}^{(1)} + \mathcal{H}^{(2)} = & \mathcal{E}\hat{I} + \sum_A \mathcal{Z}_A \hat{Z}_A + \mathcal{X}_A \hat{X}_A \\ & + \sum_{A>B} \mathcal{X} \mathcal{X}_{AB} \hat{X}_A \otimes \hat{X}_B + \mathcal{X} \mathcal{Z}_{AB} \hat{X}_A \otimes \hat{Z}_B \\ & + \mathcal{Z} \mathcal{X}_{AB} \hat{Z}_A \otimes \hat{X}_B + \mathcal{Z} \mathcal{Z}_{AB} \hat{Z}_A \otimes \hat{Z}_B. \end{aligned} \quad (8)$$

The choice of Hamiltonian matrix elements $\{\mathcal{Z}_A, \mathcal{X}_A, \mathcal{Z}\mathcal{Z}_{AB}, \mathcal{Z}\mathcal{X}_{AB}, \mathcal{X}\mathcal{Z}_{AB}, \mathcal{X}\mathcal{X}_{AB}\}$ for a given photoactive complex is an interesting art. Choosing these parameters empirically to match experiment or other reference data is the crux of the phenomenological Frenkel-Davydov exciton model [64,65]. Recently, we introduced a new *ab initio* exciton model approach [45–49], in which the parameters of the exciton model are determined explicitly by high-level *ab initio* computations on the isolated monomers, under the assumption of sufficient monomer separations to relax the fermionic antisymmetry constraint. We have extended the *ab initio* exciton model to treat full nonadiabatic dynamics through the development of analytical gradients or coupling vectors [46,47] and have increased the basis set to include both local and charge-transfer excitations [47].

In this *ab initio* exciton model, the Hamiltonian matrix elements in Eq. (8) all have distinct physical origins: \mathcal{E} is the mean-field energy, \mathcal{Z}_A is roughly (half) of the difference between the ground- and excited-state energy of monomer A , $\mathcal{X}\mathcal{X}_{AB}$ is the transition-dipole–transition-dipole interaction and $\mathcal{Z}\mathcal{Z}_{AB}$ is the difference-dipole–difference-dipole interaction between monomers A and B , and $\mathcal{X}\mathcal{Z}_{AB}$ and $\mathcal{Z}\mathcal{X}_{AB}$ are transition-dipole–difference-dipole interaction cross terms. \mathcal{Z}_A and \mathcal{X}_A carry Fock-matrix like dressings from the mean-field electrostatic environment of the system. A full definition of the matrix elements is available in the Supplemental Material [56].

Diagonalizing this Hamiltonian to obtain the eigenstates $\{|\Psi_\Theta\rangle\}$, even for a model of this simplicity, is difficult classically due to the 2^N dimension of the Hilbert space $|p_0\rangle \otimes |q_1\rangle \otimes \dots \otimes |r_{N-1}\rangle$. To highlight this, we point out that this part of the problem is usually solved classically in a highly restricted Hilbert space where only single excitations are allowed [45–47]: for many energy-transfer applications this may be reasonable, but will be incapable of describing the conical intersection between the ground and lowest-excited states [66]. However, it is apparent that the *ab initio* exciton Hamiltonian is entirely isomorphic to an extended spin-lattice Hamiltonian. Therefore, existing technologies for the quantum simulation of spin-lattice Hamiltonians should provide utility for this problem.

Below, we demonstrate the potential for this mapping by simulating the quantum computation of the absorption spectrum of a large photoactive complex using MC-VQE. Note that we are not the first to propose a crossover between exciton models for photoactive complexes and spin-lattice models in qubits: there have been myriad prior studies using phenomenological exciton models to theoretically characterize [67–69] or physically simulate [70–73] the exciton energy transfer (EET) process in open systems such as the Fenna-Matthews-Olsen complex. However, the emphasis in the prior literature has been on the modeling of the dissipative nonadiabatic dynamics of EET through coupling with the protein or solvent environment in an effective way (via effective phonon coupling approaches such as the Holstein model). In our approach, we emphasize the accurate *ab initio* computation of the electronic absorption spectrum at a given nuclear configuration, as a prerequisite for direct nonadiabatic dynamics simulations.

Demonstration.—MC-VQE circuits were implemented in our in-house quantum simulator package, QUASAR. All aspects of state preparation, VQE entanglement, and casting of transition matrix elements as difference observables were performed in the simulator, though one- and two-body Pauli expectation values were evaluated through contractions of wave function amplitudes (equivalent to infinite averaging of discrete Pauli measurements), and noise or error channels were not modeled. CIS is solved classically on the basis of the reference and all singly excited configurations. We avoid the “barren plateaus” issue of locating optimized VQE parameters [74] by finding a tightly converged and near-global-optimal solution for the 108 MC-VQE parameters which is directly downhill from a zero-entanglement guess in 14 L-BFGS iterations, using finite-difference gradients [56].

For a practical test case, an *ab initio* exciton model was constructed for the $N = 18$ cyclical LH2 B850 ring complex of the purple photosynthetic bacteria—the specific geometry is provided in the Supplemental Material [56]. Monomer Hamiltonian matrix elements were computed in the graphical processing unit (GPU)-accelerated TERACHEM program [75–77] for classical electronic structure theory, using TDA-TD-DFT [4] at ω PBE($\omega = 0.3$)/6-31G* [78,79]. Dimer Hamiltonian matrix elements were approximated by the dipole–transition-dipole model. Dimer Hamiltonian matrix elements were truncated after cyclical nearest-neighbor contacts due to the r_{AB}^{-3} decay of the interactions. Figure 2 depicts the simulated absorption spectrum of this *ab initio* exciton model computed from the excitation energies and oscillator strengths of the lowest 18 electronic transitions with MC-VQE and CIS, and compared to the “full configuration interaction” (FCI) reference computed in the space of all possible 2^N monomer excitation configurations. The CIS absorption shows a noticeable blue shift of a few hundredths of an eV relative

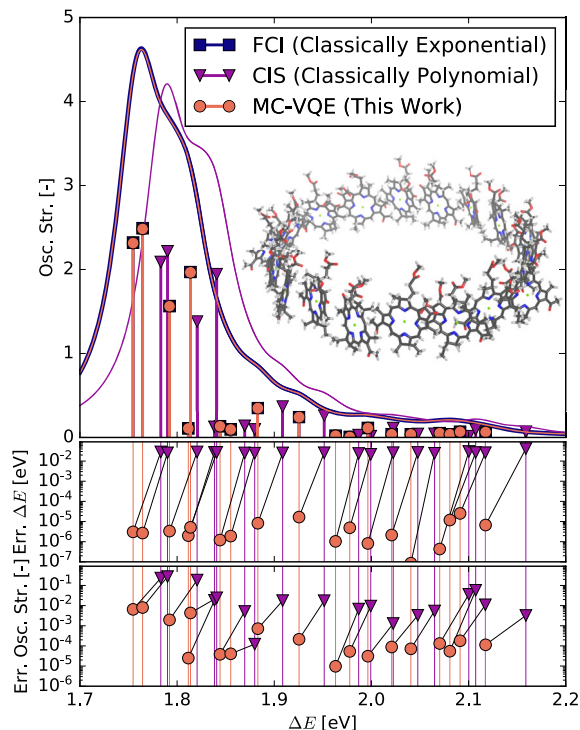


FIG. 2. Top—simulated absorption spectrum of $N = 18$ cyclical LH2 B850 ring complex (geometry depicted in inset), computed from the excitation energies and oscillator strengths of the lowest 18 electronic transitions, depicted as vertical sticks. The envelope of the absorption spectrum is sketched by broadening the contribution from each transition with a Lorentzian with width of $\delta = 0.05$ eV. The simulated MC-VQE and reference FCI results are visually indistinguishable. Middle—errors in excitation energies. Bottom—errors in oscillator strengths. Middle and bottom—thin lines are a guide for the eye.

to FCI, and, more noticeably, the CIS oscillator strengths may deviate by 10% or more, particularly for the brightest states. By contrast, MC-VQE with a single entangler layer is visually indistinguishable from FCI—the maximum deviations of excitation energies are on the order of tens of μ eV, while the oscillator strengths generally deviate by $\ll 1\%$. At the request of a reviewer, we have also considered a test case where CIS produces qualitatively incorrect results relative to FCI: an $N = 8$ linear stack of BChl-a chromophores. MC-VQE has no trouble with this system and again produces results which are essentially visually indistinguishable from FCI; see the Supplemental Material [56] for full details.

Outlook.—In this Letter, we have demonstrated a hybrid quantum or classical approach for the modeling of electronic absorption spectra in large-scale photoactive complexes by using a multistate, contracted variant of VQE (MC-VQE) in the context of an *ab initio* exciton model. We simulated MC-VQE for an $N = 18$ LH2 B850 complex (a Hilbert space dimension of $2^{18} = 262144$). The MC-VQE absorption spectrum matches FCI quantitatively with only a single layer of VQE two-body entanglers with a

connectivity matching that of the exciton Hamiltonian. With a qubit count equivalent to the number of monomers N , a circuit depth that is linear in N , a gate count that is quadratic in N , and a requirement of only one- and a sparse set of two-body Pauli measurements, MC-VQE applied to an *ab initio* exciton model with local Hamiltonian connectivity is a compelling application for deployment to near-term quantum hardware.

This Letter is intended to sketch the salient features of the MC-VQE algorithm and its potential application to the *ab initio* exciton model. Future work will investigate robustness of the algorithm on realistic hardware including the influence of gate and measurement errors. *Ab initio* exciton Hamiltonians with more-complicated local connectivity that are unlikely to be addressable with classical methods such as DMRG should also be investigated. Beyond this, effort should be devoted to direct implementation on real hardware, where circuit locality and simplification or sparsification will be of key importance. Finally, MC-VQE should be explored in the context of direct simulation of fermionic electronic structure problems—it seems highly likely that this algorithm will be easily adaptable to the study of multiple excited states in many types of Hamiltonians beyond the *ab initio* exciton model.

This material is based on work partially supported by the U.S. Department of Energy, Office of Science, Office of Advanced Scientific Computing Research (SciDAC) program.

Financial disclosure.—T. J. M. is a cofounder of PetaChem LLC. R. M. P. and P. L. M. own stock or options in QC Ware Corp.

Note added.—Recently we learned of the “subspace search” VQE (SSVQE) approach developed by Nakanishi, Mitarai, and Fujii in a preprint [80]. Both SSVQE and MC-VQE use a state-averaged VQE entangler \hat{U} , and both describe how to compute transition properties. The methods have several key differences: SSVQE uses hybrid quantum-classical optimization to determine the minimal and maximal eigenvectors in the subspace matrix, while MC-VQE uses classical diagonalization of the subspace Hamiltonian to determine all subspace eigenstates simultaneously. Additionally, MC-VQE uses contracted reference states (e.g., from CIS), while SSVQE uses Hilbert-space configurations.

*rob.parrish@qcware.com

- [1] T. Helgaker, P. Jørgensen, and J. Olsen, *Molecular Electronic Structure Theory* (Wiley, New York, 2000).
- [2] P. Hohenberg and W. Kohn, *Phys. Rev.* **136**, B864 (1964).
- [3] W. Kohn and L. J. Sham, *Phys. Rev.* **140**, A1133 (1965).
- [4] E. Runge and E. K. U. Gross, *Phys. Rev. Lett.* **52**, 997 (1984).

- [5] W. Koch and M. C. Holthausen, *A Chemist’s Guide to Density Functional Theory* (Wiley-VCH, New York, 2001).
- [6] J. Cížek, *J. Chem. Phys.* **45**, 4256 (1966).
- [7] G. D. Purvis and R. J. Bartlett, *J. Chem. Phys.* **76**, 1910 (1982).
- [8] T. D. Crawford and H. F. Schaefer, *An Introduction to Coupled Cluster Theory for Computational Chemists* (Wiley-Blackwell, Hoboken, 2007), pp. 33–136.
- [9] I. Shavitt and R. Bartlett, *Many-Body Methods in Chemistry and Physics: MBPT and Coupled-Cluster Theory*, Cambridge Molecular Science (Cambridge University Press, Cambridge, England, 2009).
- [10] S. R. White, *Phys. Rev. Lett.* **69**, 2863 (1992).
- [11] G. K.-L. Chan and S. Sharma, *Annu. Rev. Phys. Chem.* **62**, 465 (2011).
- [12] C. F. Bender and E. R. Davidson, *Phys. Rev.* **183**, 23 (1969).
- [13] B. Huron, J. Malrieu, and P. Rancurel, *J. Chem. Phys.* **58**, 5745 (1973).
- [14] G. H. Booth, A. J. Thom, and A. Alavi, *J. Chem. Phys.* **131**, 054106 (2009).
- [15] D. Cleland, G. Booth, and A. Alavi, *J. Chem. Phys.* **132**, 041103 (2010).
- [16] A. A. Holmes, N. M. Tubman, and C. Umrigar, *J. Chem. Theory Comput.* **12**, 3674 (2016).
- [17] J. B. Schriber and F. A. Evangelista, *J. Chem. Phys.* **144**, 161106 (2016).
- [18] J. B. Schriber and F. A. Evangelista, *J. Chem. Theory Comput.* **13**, 5354 (2017).
- [19] J. E. Deustua, J. Shen, and P. Piecuch, *Phys. Rev. Lett.* **119**, 223003 (2017).
- [20] J. E. Deustua, I. Magoulas, J. Shen, and P. Piecuch, *J. Chem. Phys.* **149**, 151101 (2018).
- [21] D. S. Abrams and S. Lloyd, *Phys. Rev. Lett.* **79**, 2586 (1997).
- [22] D. S. Abrams and S. Lloyd, *Phys. Rev. Lett.* **83**, 5162 (1999).
- [23] A. Aspuru-Guzik, A. D. Dutoi, P. J. Love, and M. Head-Gordon, *Science* **309**, 1704 (2005).
- [24] B. P. Lanyon *et al.*, *Nat. Chem.* **2**, 106 (2010).
- [25] D. Wecker, B. Bauer, B. K. Clark, M. B. Hastings, and M. Troyer, *Phys. Rev. A* **90**, 022305 (2014).
- [26] N. M. Tubman *et al.*, arXiv:1809.05523.
- [27] A. Peruzzo, J. McClean, P. Shadbolt, M.-H. Yung, X.-Q. Zhou, P. J. Love, A. Aspuru-Guzik, and J. L. O’Brien, *Nat. Commun.* **5**, 4213 (2014).
- [28] J. R. McClean, J. Romero, R. Babbush, and A. Aspuru-Guzik, *New J. Phys.* **18**, 023023 (2016).
- [29] P. OMalley *et al.*, *Phys. Rev. X* **6**, 031007 (2016).
- [30] A. Kandala, A. Mezzacapo, K. Temme, M. Takita, M. Brink, J. M. Chow, and J. M. Gambetta, *Nature (London)* **549**, 242 (2017).
- [31] J. R. McClean *et al.*, arXiv:1710.07629.
- [32] J. Romero *et al.*, *Quant. Sci. Tech.* **4**, 014008 (2018).
- [33] P. Jordan and E. Wigner, *Z. Phys.* **47**, 631 (1928).
- [34] G. Ortiz, J. E. Gubernatis, E. Knill, and R. Laflamme, *Phys. Rev. A* **64**, 022319 (2001).
- [35] S. B. Bravyi and A. Y. Kitaev, *Ann. Phys. (Amsterdam)* **298**, 210 (2002).
- [36] J. T. Seeley, M. J. Richard, and P. J. Love, *J. Chem. Phys.* **137**, 224109 (2012).

- [37] K. Setia and J. D. Whitfield, [arXiv:1712.00446](https://arxiv.org/abs/1712.00446).
- [38] K. Setia, S. Bravyi, A. Mezzacapo, and J. D. Whitfield, [arXiv:1810.05274](https://arxiv.org/abs/1810.05274).
- [39] R. Babbush, N. Wiebe, J. McClean, J. McClain, H. Neven, and G. Kin-Lic Chan, *Phys. Rev. X* **8**, 011044 (2018).
- [40] I. D. Kivlichan, J. McClean, N. Wiebe, C. Gidney, A. Aspuru-Guzik, G. Kin-Lic Chan, and R. Babbush, *Phys. Rev. Lett.* **120**, 110501 (2018).
- [41] M. Motta *et al.*, [arXiv:1808.02625](https://arxiv.org/abs/1808.02625).
- [42] E. G. Hohenstein, R. M. Parrish, and T. J. Martínez, *J. Chem. Phys.* **137**, 044103 (2012).
- [43] R. M. Parrish, E. G. Hohenstein, T. J. Martínez, and C. D. Sherrill, *J. Chem. Phys.* **137**, 224106 (2012).
- [44] R. M. Parrish, E. G. Hohenstein, N. F. Schunck, C. D. Sherrill, and T. J. Martínez, *Phys. Rev. Lett.* **111**, 132505 (2013).
- [45] A. Sisto, D. R. Glowacki, and T. J. Martinez, *Acc. Chem. Res.* **47**, 2857 (2014).
- [46] A. Sisto, C. Stross, M. W. van der Kamp, M. O'Connor, S. McIntosh-Smith, G. T. Johnson, E. G. Hohenstein, F. R. Manby, D. R. Glowacki, and T. J. Martinez, *Phys. Chem. Chem. Phys.* **19**, 14924 (2017).
- [47] X. Li, R. M. Parrish, F. Liu, S. I. Kokkila Schumacher, and T. J. Martínez, *J. Chem. Theory Comput.* **13**, 3493 (2017).
- [48] A. F. Morrison, Z.-Q. You, and J. M. Herbert, *J. Chem. Theory Comput.* **10**, 5366 (2014).
- [49] A. F. Morrison and J. M. Herbert, *J. Phys. Chem. Lett.* **6**, 4390 (2015).
- [50] R. Santagati *et al.*, *Sci. Adv.* **4**, eaap9646 (2018).
- [51] S. Endo, T. Jones, S. McArdle, X. Yuan, and S. Benjamin, [arXiv:1806.05707](https://arxiv.org/abs/1806.05707).
- [52] O. Higgott, D. Wang, and S. Brierley, [arXiv:1805.08138](https://arxiv.org/abs/1805.08138).
- [53] J. Lee, W. J. Huggins, M. Head-Gordon, and K. B. Whaley, *J. Chem. Theory Comput.* **15**, 311 (2018).
- [54] J. R. McClean, M. E. Kimchi-Schwartz, J. Carter, and W. A. de Jong, *Phys. Rev. A* **95**, 042308 (2017).
- [55] J. I. Colless, V. V. Ramasesh, D. Dahlen, M. S. Blok, M. E. Kimchi-Schwartz, J. R. McClean, J. Carter, W. A. de Jong, and I. Siddiqi, *Phys. Rev. X* **8**, 011021 (2018).
- [56] See Supplemental Material at <http://link.aps.org/supplemental/10.1103/PhysRevLett.122.230401> for detailed derivation and definition of the Hamiltonian matrix elements, for technical details of the CIS state preparation, MC-VQE entangler circuits, and output of the MC-VQE optimization profile, and for an additional case study with increased multiexcitonic character.
- [57] F. Diker, [arXiv:1606.09290](https://arxiv.org/abs/1606.09290).
- [58] J. Zhang, J. Vala, S. Sastry, and K. B. Whaley, *Phys. Rev. Lett.* **91**, 027903 (2003).
- [59] V. V. Shende, I. L. Markov, and S. S. Bullock, *Phys. Rev. A* **69**, 062321 (2004).
- [60] F. Vatan and C. Williams, *Phys. Rev. A* **69**, 032315 (2004).
- [61] H.-R. Wei and Y.-M. Di, [arXiv:1203.0722](https://arxiv.org/abs/1203.0722).
- [62] P. Durand, *Phys. Rev. A* **28**, 3184 (1983).
- [63] D. Maynau, P. Durand, J. P. Daudey, and J. P. Malrieu, *Phys. Rev. A* **28**, 3193 (1983).
- [64] J. Frenkel, *Phys. Rev.* **37**, 17 (1931).
- [65] A. S. Davydov, *Phys. Usp.* **7**, 145 (1964).
- [66] B. G. Levine, C. Ko, J. Quenneville, and T. J. Martínez, *Mol. Phys.* **104**, 1039 (2006).
- [67] M. B. Plenio and S. F. Huelga, *New J. Phys.* **10**, 113019 (2008).
- [68] F. Caruso, A. W. Chin, A. Datta, S. F. Huelga, and M. B. Plenio, *J. Chem. Phys.* **131**, 105106 (2009).
- [69] F. Caruso, A. W. Chin, A. Datta, S. F. Huelga, and M. B. Plenio, *Phys. Rev. A* **81**, 062346 (2010).
- [70] S. Mostame, P. Rebentrost, A. Eisfeld, A. J. Kerman, D. I. Tsomokos, and A. Aspuru-Guzik, *New J. Phys.* **14**, 105013 (2012).
- [71] S. Mostame, J. Huh, C. Kreisbeck, A. J. Kerman, T. Fujita, A. Eisfeld, and A. Aspuru-Guzik, *Quantum Inf. Process.* **16**, 44 (2017).
- [72] A. Potočník *et al.*, *Nat. Commun.* **9**, 904 (2018).
- [73] B.-X. Wang *et al.*, [arXiv:1801.09475](https://arxiv.org/abs/1801.09475).
- [74] J. R. McClean, S. Boixo, V. N. Smelyanskiy, R. Babbush, and H. Neven, *Nat. Commun.* **9**, 4812 (2018).
- [75] I. S. Ufimtsev and T. J. Martinez, *J. Chem. Theory Comput.* **5**, 2619 (2009).
- [76] N. Luehr, I. S. Ufimtsev, and T. J. Martínez, *J. Chem. Theory Comput.* **7**, 949 (2011).
- [77] C. M. Isborn, A. W. Gotz, M. A. Clark, R. C. Walker, and T. J. Martínez, *J. Chem. Theory Comput.* **8**, 5092 (2012).
- [78] Y. Tawada, T. Tsuneda, S. Yanagisawa, T. Yanai, and K. Hirao, *J. Chem. Phys.* **120**, 8425 (2004).
- [79] O. A. Vydrov and G. E. Scuseria, *J. Chem. Phys.* **125**, 234109 (2006).
- [80] K. M. Nakanishi, K. Mitarai, and K. Fujii, [arXiv:1810.09434](https://arxiv.org/abs/1810.09434).